Experimental therapy of malignant gliomas using the inhibitor of histone deacetylase MS-275

Ilker Y. Eyüpoglu,[1] Eric Hahnen,[2,3] Christian Tränkle,[4] Nicolai E. Savaskan,[5] Florian A. Siebzehnrübl,[2] Rolf Buslei,[2] Dieter Lemke,[6] Wolfgang Wick,[6] Rudolf Fahlbusch,[1] and Ingmar Blümcke[2]

Departments of [1]Neurosurgery and [2]Neuropathology, University of Erlangen-Nuremberg, Erlangen-Nuremberg, Germany; [3]Institute of Human Genetics, Institute of Genetics, and Center for Molecular Medicine Cologne, University of Cologne, Cologne, Germany; [4]Department of Pharmacology and Toxicology, Institute of Pharmacy, University of Bonn, Bonn, Germany; [5]Division of Cellular Biochemistry, The Netherlands Cancer Institute, Amsterdam, the Netherlands; and [6]Department of General Neurology, Hertie Institute for Clinical Brain Research, University of Tübingen, Tübingen, Germany

Abstract

Inhibitors of histone deacetylases are promising compounds for the treatment of cancer but have not been systematically explored in malignant brain tumors. Here, we characterize the benzamide MS-275, a class I histone deacetylase inhibitor, as potent drug for experimental therapy of glioblastomas. Treatment of four glioma cell lines (U87MG, C6, F98, and SMA-560) with MS-275 significantly reduced cell growth in a concentration-dependent manner (IC_{90}, 3.75 μmol/L). Its antiproliferative effect was corroborated using a bromodeoxyuridine proliferation assay and was mediated by G_0-G_1 cell cycle arrest (i.e., up-regulation of p21/WAF) and apoptotic cell death. Implantation of enhanced green fluorescent protein–transfected F98 glioma cells into slice cultures of rat brain confirmed the cytostatic effect of MS-275 without neurotoxic damage to the organotypic neuronal environment in a dose escalation up to 20 μmol/L. A single intratumoral injection of MS-275 7 days after orthotopic implantation of glioma cells in syngeneic rats confirmed the chemotherapeutic efficacy of MS-275 *in vivo*. Furthermore, its propensity to pass the blood-brain barrier and to increase the protein level of acetylated histone H3 in brain tissue identifies MS-275 as a promising candidate drug in the treatment of malignant gliomas. [Mol Cancer Ther 2006;5(5):1248–55]

Introduction

Acetylation and deacetylation of core histones are key regulatory mechanisms of gene expression (1). Whereas histone acetylation seems to relax the chromatin structure, thereby promoting gene transcription, histone deacetylation induces a repressive environment mediated by chromatin condensation. In addition, normal cell differentiation and adjustment of metabolic activity require coordinated gene transcription and balanced activity of histone acetyltransferases versus histone deacetylases (HDAC; ref. 2). This assumption is supported by the finding that deletions or inactivating mutations of histone acetyltransferase are associated with tumor progression in humans (3, 4). The propensity to block HDAC activities by specific inhibitors provides the intriguing opportunity to pharmacologically modulate gene transcription by epigenetic regulation and may counteract the described dysbalance. Various HDAC inhibitors have been identified as promising compounds for the treatment of cancer, either alone (5, 6) or in combination with other agents (6–8). These novel compounds induce growth arrest and apoptotic cell death in a variety of transformed cells (9, 10). Molecular pathways induced by HDAC inhibitors and which either accelerate cellular maturation or cell death remain to be determined. However, epigenetic modifiers of gene expression exert their beneficial effect in the treatment of central nervous system tumors (e.g., malignant gliomas) by up-regulation of cell cycle regulator proteins (i.e., p21/WAF and gelsolin; refs. 5, 11, 12) or initiation of apoptosis mechanisms in glioma cells (12–14). Moreover, *in vitro* experiments with leukemia cells have shown that HDAC inhibitors are able to induce expression of death receptors, which result in enhanced activity of caspase-8 or cleavage of Bid (15, 16). Furthermore, HDAC inhibitors are able to disrupt cellular redox state (e.g., reactive oxygen species; refs. 9, 17, 18), damage function of heat shock proteins (e.g., acetylation of heat shock protein 90; ref. 19), and down-regulate survival signaling pathways (15, 20).

Despite multimodal therapy regimens, including radical neurosurgical resection, radiotherapy, and polychemotherapy, the response of malignant gliomas remains poor (21) and patients experience a median survival of 12 months from the time point of diagnosis (22, 23). Recently, the DNA alkylating drug temozolomide seems to increase survival in ~20% of patients (24, 25). This success will foster the identification of novel chemotherapeutic compounds,

Received 12/20/05; revised 2/7/06; accepted 3/2/06.

Grant support: ELAN-Fonds of the University of Erlangen-Nuremberg (I.Y. Eyüpoglu and I. Blümcke), ''Nolting Stiftung'' (E. Hahnen), Human Frontiers Science Program (N.E. Savaskan), and German Research Council (DFG SA 1041/2-3; N.E. Savaskan).

The costs of publication of this article were defrayed in part by the payment of page charges. This article must therefore be hereby marked advertisement in accordance with 18 U.S.C. Section 1734 solely to indicate this fact.

Note: I.Y. Eyüpoglu and E. Hahnen contributed equally as first authors.

Requests for reprints: Ilker Y. Eyüpoglu, Department of Neurosurgery, University of Erlangen-Nuremberg, Schwabachanlage 6, 91054 Erlangen, Germany. Phone: 49-9131-85-34418; Fax: 49-9131-85-26033. E-mail: eyupoglu@gmx.net

doi:10.1158/1535-7163.MCT-05-0533

which would then rapidly translate into clinical perspectives. HDAC inhibitors may offer this opportunity. MS-275 has entered clinical phase I trial for the treatment of solid tumors and lymphoma (26, 27). It potently triggers the early release of reactive oxygen species and induces mitochondrial damage in various cancer cell lines (9, 17). Here, we analyze the therapeutic potential of MS-275 to reduce glioma progression in monolayer cultures, an organotypic glioma invasion model using entorhino-hippocampal slice cultures of rat brain, as well as *in vivo* following single intrathecal injection of MS-275 7 days after implantation of glioma cells into rat brain.

Materials and Methods

Monolayer Culture

The rat glioma cell line F98 was established from ethylnitrosourea-induced carcinogenesis in CDF Fisher rats (28). The human glioma cell line U87MG (29) and the rat glioma cell line C6 (30) were obtained from the American Type Culture Collection (Manassas, VA). SMA-560 mouse glioma cells (31) were kindly provided by D.D. Bigner (Durham, NC). All glioma cell lines were cultivated in a humidified atmosphere at 37°C and 5% CO_2 using culture conditions and medium as recommended by the supplier.

Chemicals

N-(2-aminophenyl)-4-[*N*-(pyridine-3-ylmetoxycarbonyl)aminomethyl]benzamide (MS-275) was obtained from Calbiochem (Bad Soden, Germany). Temozolomide was supplied by Schering-Plough (Kenilworth, NJ). Both compounds were dissolved in DMSO (Sigma-Aldrich, Munich, Germany) and diluted in medium before experimental use.

Microscopic Evaluation

Morphometric analysis was done using high-power optical fields digitized with a CCD camera (Color View II, Soft Imaging System, Münster, Germany) equipped to a BX51 microscope (Olympus, Tokyo Japan) and respective imaging software (analySIS, Soft Imaging System, Stuttgart, Germany). Fluorescence-labeled tumor cells transplanted to organotypic brain slice cultures as well as propidium iodide (PI) staining intensities (see below) were analyzed by an Olympus microscope (IX 70) equipped with a TRITC (excitation filter 520–550 nm, barrier filter 580 nm) and FITC (excitation filter 450–490 nm, band filter 520–550) narrow band filter, a CCD camera (F-View II), and respective image software (analySIS). Statistical significance was calculated with Student's *t* test (StatView II, Abacus).

3-(4,5-Dimethylthiazol-2-yl)-2,5-Diphenyltetrazolium Bromide and Bromodeoxyuridine Proliferation Assays

Viable cell numbers were estimated by 3-(4,5-dimethylthiazol-2-yl)-2,5-diphenyltetrazolium bromide assay. Cells (8,000/mL) were seeded in a 96-well plate (final volume, 250 μL/well). One hour after seeding, the cells were treated with either MS-275, temozolomide, or solvent. Medium was changed after 48 hours. At 96 hours after incubation, 0.5 mg/mL 3-(4,5-dimethylthiazol-2-yl)-2,5-diphenyltetrazolium bromide (Sigma-Aldrich) dissolved in medium was applied for 2 hours. Subsequently, the medium was discarded and each well was incubated with 100 μL of an isopropanol stock solution containing 165 μL hydrochloric acid/50 mL isopropanol. The absorbance of each well was subsequently determined using a microplate reader (Tecan, Crailsheim, Germany) set to 550 nm (wavelength correction set to 690 nm). The proliferation of F98 glioma cells was analyzed using the Bromodeoxyuridine Labeling and Detection Kit III according to the manufacturer's protocol (Roche, Mannheim, Germany).

Measurement of HDAC Activity

HDAC activity was determined by applying a BioVision fluorimetric assay (BioCat, Heidelberg, Germany; ref. 32). Fluorescence signal was measured with a NOVOstar plate reader (BMG Labtech, Offenburg, Germany) at excitation wavelength of 380 nm and emission wavelength of 460 nm. Rat liver HDAC was purchased from Alexis Biochemicals (Grünberg, Germany); 30 μL of the stock preparation were applied per well; its specific HDAC activity amounted to ~100 pmol substrate/min at 37°C. Trichostatin A (1 mmol/L) was used as a positive control.

Data Analysis

Concentration-effect curves for the inhibition of cell viability and HDAC activity following drug treatment were calculated by nonlinear regression analysis using GraphPad Prism version 4.00 for Windows (GraphPad, San Diego, CA). Data were fitted to a four-variable logistic equation comprising the top plateau, bottom plateau, inflection point IC_{50}, and curve slope n_H. The variables IC_{50} and n_H and ''bottom'' were set as variables and ''top'' was the control value of cell viability or HDAC activity, respectively, and was set constant at 100%. It was tested successively, whether the slope n_H or the bottom plateau was different from unity or zero (*F* test). Cell viability approached zero in the presence of high concentrations of the test compounds and extended incubation times. Therefore, the variable ''bottom'' was set at constant = 0 in the respective nonlinear regression analyses.

Protein Preparation and Immunoblotting

F98 glioma cells were treated with either MS-275 or solvent. After 24 hours, cells were pelleted by centrifugation at 175 × *g* for 10 minutes and the supernatant fraction was decanted. Cells were washed with PBS and suspended in lysis buffer [10 mmol/L HEPES (pH 7.9), 1.5 mmol/L $MgCl_2$, 10 mmol/L KCl, 0.5 mmol/L DTT, 1.5 mmol/L phenylmethylsulfonyl fluoride]. Sulfuric acid was added to a final concentration of 0.2 mol/L. The cells were incubated for 30 minutes on ice and centrifuged at 10,080 × *g* for 10 minutes at 4°C. The supernatant fraction was dialyzed against 200 mL of 0.1 mol/L acetic acid for 2 hours and dialyzed again thrice against 200 mL H_2O (1 and 3 hours and overnight). Supernatant was subjected to SDS-PAGE on a 12% polyacrylamide gel. The soluble fraction (10 μg) was loaded per lane. The separated proteins were electroblotted onto nitrocellulose (Sigma-Aldrich). Equal loading amounts of the probes were estimated using immunostaining with an anti-mouse β-actin monoclonal antibody

(Sigma-Aldrich). Controls and treated F98 cells were analyzed for nonacetylated and acetylated histone H3 with polyclonal antibodies (Biomol, Hamburg, Germany) and chemiluminescence detection method (Amersham, Freiburg, Germany).

Flow Cytometry

F98 cells were treated with an ice-cold hypotonic solution of PI (Sigma-Aldrich) for 30 minutes in the dark. Adherent and floating cells were included and the rate of apoptosis and cell cycle distribution were analyzed using flow cytometry (FACSCalibur, BD Biosciences, Heidelberg, Germany).

Transfection of Enhanced Green Fluorescent Protein into F98 Glioma Cells

F98 cells were transfected with pEGFP-N1 (BD Biosciences Clontech, Erembodegem, Belguim) using calcium phosphate coprecipitation. Briefly, cells were plated in 1.9 cm^2 dishes at a density of 20,000 per well in 500 μL culture medium. Twenty-four hours later, the medium was discarded and 500 μL DNA precipitate/well was added to the cells. The DNA precipitate was generated by adding 417.5 μL sterile water, 62.5 μL of 2 mol/L $CaCl_2$, 20 μg plasmid DNA, 500 μL BES buffer (containing 1.07 g BES; Sigma-Aldrich), 1.63 g NaCl, and 0.0267 g $Na_2HPO_4{\cdot}2H_2O$ in 100 mL sterile water at pH 6.95 into a final volume of 10 mL culture medium. Cells were incubated for 20 hours at 37°C and 5% CO_2. Precipitate-containing medium was removed and the cells were cultured in the primary culture medium for 24 hours. Transfected cells were cultured in a selection medium (containing 500 μg/mL G418; Sigma-Aldrich) for 4 weeks.

Organotypic Entorhino-Hippocampal Slice Cultures

Slice cultures were prepared and maintained as described (33). Seven-day-old Wistar rats were used for explantation. After decapitation, the brains were removed and placed into preparation medium containing HBSS (Life Technologies, Karlsruhe, Germany) with 10% normal horse serum (Biochrom, Berlin, Germany). The brains were cut in 350-μm-thick horizontal slices using a vibratome (Leica VT 1000S, Bensheim, Germany). Slices were transferred into culture plate insert membrane dishes (Becton Dickinson, Franklin Lakes, NJ; pore size, 0.4 μm) and subsequently transferred into six-well culture dishes (Becton Dickinson) containing 1.2 mL culture medium (2:1 MEM/HBSS, 25% normal horse serum, 2% L-glutamine, 2.64 mg/mL glucose, 100 units/mL penicillin, 0.1 mg/mL streptomycin, 10 μg/mL insulin-transferrin-sodium selenite supplement, and 0.8 μg/mL vitamin C) according to the interface technique (34). Slices were cultured in humidified atmosphere at 35°C and 5% CO_2. Medium was changed 1 day after preparation and every second day thereafter.

Neurotoxicity in Organotypic Entorhino-Hippocampal Slice Cultures

Slice cultures were incubated with 1 μg/mL PI for 20 minutes followed by complete medium exchange to visualize irreversibly damaged cell bodies. Neurotoxicity was evaluated using an inverse fluorescence microscope (see details above) and respective documentation software (analySIS).

Organotypic Glioma Invasion Model

Five thousand enhanced green fluorescent protein–positive F98 glioma cells were implanted within a total volume of 0.1 μL medium into the entorhinal cortex 1 day after slice preparation (35). One day after implantation and every second day, glioma growth and invasion were evaluated using an inverse fluorescence microscope (see details above).

Glioma Implantation *In vivo*

F98 rat glioma cells (5×10^3) were stereotactically implanted into the right striatum of 12 Fisher rats weighting 200 g (Charles River, Sulzfeld, Germany). Six rats were locally injected at day 7 with 10 μL DMSO vehicle or 10 μL of a 10 μmol/L MS-275 solution into the transplantation site. Neurologic deficits were scored daily [grade 0, normal; grade 1, tail weakness or tail paralysis; grade 2, hind leg paraparesis or hemiparesis; grade 3, hind leg paralysis or hemiparalysis; grade 4, complete paralysis (tetraplegia), moribund stage, or death; ref. 36]. All animals were sacrificed after the first rat showed tetraplegia and brains were collected for standard histologic procedures. All animal work was carried out in accordance with the NIH *Guide for the Care and Use of Laboratory Animals* and §8, section 1 of the Law for Treatment of Animals in Germany (Regierungspräsidium Tübingen, Germany). Brains were immersion fixed for 2 days using a mixture of 4% paraformaldehyde and 1% glutaraldehyde diluted in distilled water. Brains were thoroughly washed in 0.1 mol/L phosphate buffer after fixation and paraffin embedded using routine histopathologic procedures. All brains were serially sectioned at 4 μm thickness (Microm HM 335 E, Microm, Walldorf, Germany). Every 10th section was stained with H&E solution, and the extent of the tumor mass was documented by digital imaging (Color View II CCD camera and analySIS software) equipped to an Olympus BX51 microscope. The tumor masses were manually traced on the computer screen, and areas were calculated by respective imaging software (analySIS).

Brain Passage of MS-275 *In vivo*

Four C57/B6 mice (Charles River) received an i.p. injection of either 2 mg ($n = 2$) or 4 mg ($n = 2$) MS-275 dissolved in 150 μL DMSO. Two mice received DMSO only. Animals were sacrificed either after 2 hours (DMSO, 2 and 4 mg) or 4 hours (DMSO, 2 and 4 mg). The brains were removed and proteins were extracted with acid protection as described above. All animal work was carried out in accordance with the NIH *Guide for the Care and Use of Laboratory Animals* and §8, section 1 of the Law for Treatment of Animals in Germany.

Results

MS-275 Reduces Glioma Cell Growth *In vitro*

In a first set of experiments, the propensity of MS-275 to reduce glioma cell growth was analyzed *in vitro*. Four different glioma cell lines derived from different species (human U87MG, rat C6 and F98, and mouse SMA-560) were exposed to the benzamide MS-275. A sigmoidal

relationship between drug concentration and tumor cell growth was observed in all cell lines, indicating that MS-275 is highly effective at low micromolar ranges (Fig. 1A). The DNA alkylating agent temozolomide was employed to corroborate our experimental model. This drug is a clinical well-established compound in the treatment of patients suffering from malignant gliomas. To provide a proof-of-concept for the therapeutic efficacy of MS-275 in our *ex vivo* model, we compared the antiglioma efficacy of MS-275 with that of temozolomide (Fig. 1B).

In F98 cells, the equieffective concentration to reduce cell viability by 90% (IC_{90}) was 688 μmol/L for temozolomide and 3.75 μmol/L for MS-275. These results were confirmed by bromodeoxyuridine proliferation assays (Fig. 1C). We continued to characterize the HDAC-inhibiting action of MS-275 and quantified its potency to reduce HDAC activity in a cell-free system. Interestingly, MS-275 showed an incomplete inhibition of HDAC activity even at excessive concentrations (>100 μmol/L; Fig. 1D). However, the capacity of MS-275 to induce an accumulation of acetylated histones at low concentrations was shown by immunoblotting of acetylated histone H3 (data not shown). Treatment of F98 cells with IC_{90} doses of MS-275 caused a prominent increase of acetylated histone H3 protein levels after 24 hours. Moreover, incubation of F98 glioma cells with MS-275 (IC_{90} for 48 hours) induced a switch of the morphologic phenotype with outgrowth of cellular processes (data not shown). Flow cytometry of F98 glioma cells treated with MS-275 (IC_{90}) for 48 hours revealed a significant G_1 cell cycle arrest (data not shown). Following an incubation period of 72 hours, the majority of tumor cells accumulated in the sub-G_1 phase, including apoptotic DNA fragmentation (Fig. 2A and B). As shown in previous studies on HDAC inhibitor treatment in malignant tumor cell lines (9, 37), the cell cycle control protein p21/WAF was upregulated also in F98 glioma cells after MS-275 treatment (data not shown).

Neurotoxicity of MS-275 and Temozolomide in Brain Slice Cultures

In the next set of experiments, the cytotoxic effect of MS-275 was evaluated in organotypic brain environment *ex vivo*. PI uptake, which indicates irreversible cell damage, was not detectable at calculated IC_{90} concentrations for MS-275 and temozolomide. Dose escalation experiments corroborated the good tolerance of the benzamide, whereas significant cell damage was detected after administering >20-fold IC_{90} doses (80 μmol/L; Fig. 3A). In comparison, a 2-fold IC_{90} escalation of temozolomide significantly increased PI uptake in organotypic brain slice cultures (Fig. 3A and B).

MS-275 Reduces Glioma Progression in the Organotypic Glioma Invasion Model

We employed brain slice cultures also to monitor glioma proliferation and invasion within the organotypic environment (35) by implantation of enhanced green fluorescent protein–labeled F98 cells into the entorhinal cortex.

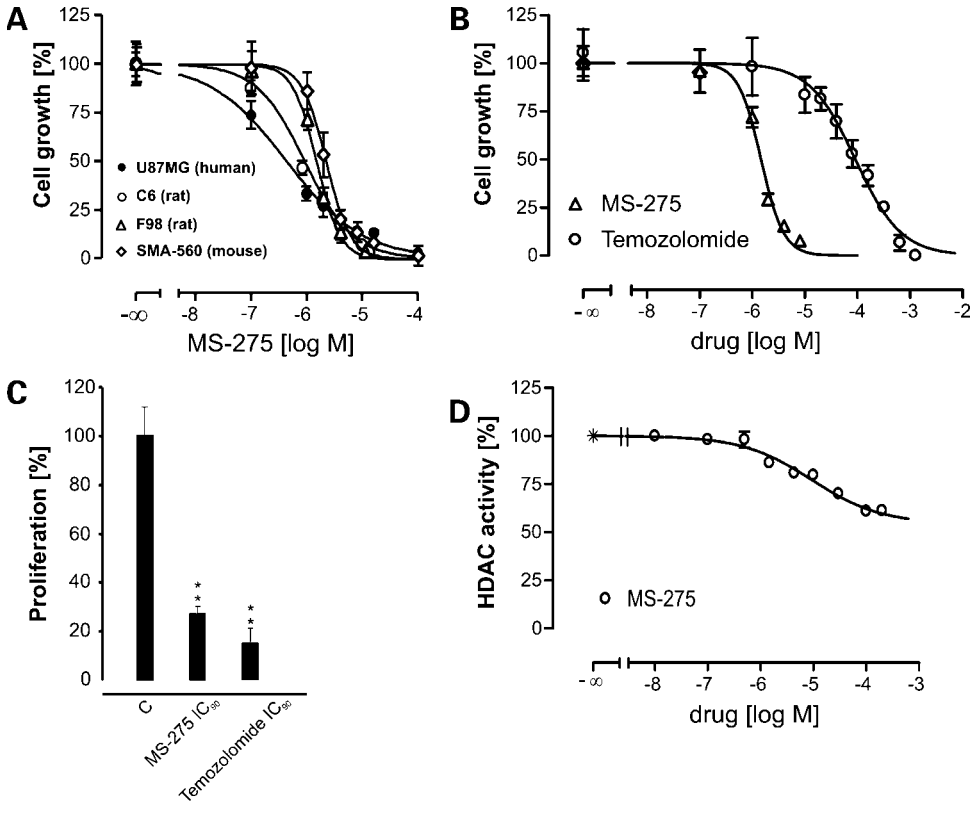

Figure 1. Concentration-dependent inhibition of cell growth. **A,** 3-(4,5-dimethylthiazol-2-yl)-2,5-diphenyltetrazolium bromide assays. *Y axis,* cell viability as a percentage of the control value in the absence of MS-275; *X axis,* log concentration of the tested compound. **B,** concentration-effect curves for the inhibitory action of MS-275 and temozolomide on cell growth calculated for F98 cells [3-(4,5-dimethylthiazol-2-yl)-2,5-diphenyltetrazolium bromide assay]. *Y* and *X* axes are similar to **A. C,** treatment with MS-275 or temozolomide significantly reduced F98 cell proliferation (bromodeoxyuridine proliferation assays; $P < 0.01$, *t* test). **D,** concentration-effect curve for the inhibition of HDAC activity by MS-275. *Y axis,* HDAC activity in percent of enzyme activity in the absence of inhibitor; *X axis,* log concentration of the tested drug. The lower plateau of the curve obtained by logistic curve fitting applying a four-variable equation was significantly different from zero and amounted to 64 ± 2% ($P < 0.05$, *F* test). The curve slope n_H for the inhibition of HDAC activity by MS-275 was not different from unity ($P > 0.05$, *F* test). Half-maximum inhibition occurred at the inflection point $pIC_{50} = 5.40 \pm 0.11$ (4 μmol/L; mean ± SE).

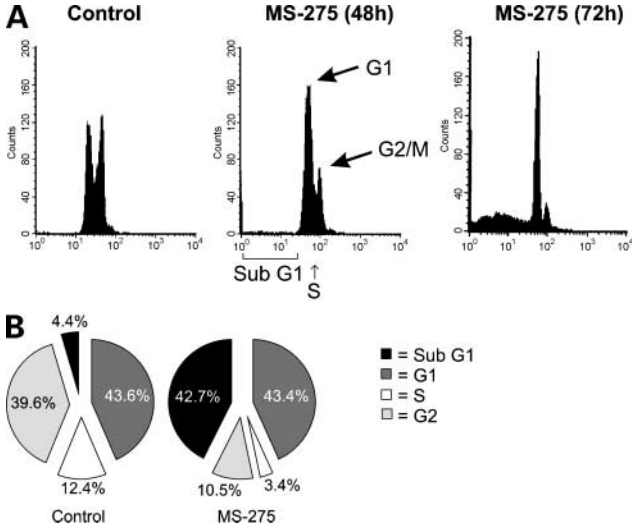

Figure 2. MS-275 induces cell cycle arrest and apoptosis. **A,** flow cytometric analysis of F98 glioma cells after 48- and 72-h exposure to MS-275 using calculated IC_{90} concentration. Sub-G_1, G_0-G_1, S, and G_2-M phases of the cell cycle. **B,** a significant accumulation in the sub-G_1 phase is observed for MS-275 treatment at 72 h ($P < 0.05$, t test) compared with time- and solvent-matched controls (data are given as percentage of cells in the different cell cycle phases).

Continuous increase of the bulk tumor mass was observed in untreated control experiments at all periods (Figs. 4 and 5). At day 5 after implantation, this increase amounted to 235% compared with the initial tumor implantation site at day 1 (defined as 100%). MS-275 and temozolomide caused a significant reduction of tumor growth 5 days after implantation as measured by fluorescence microscopy (Fig. 5A and B), whereas equieffective concentrations of temozolomide or MS-275, dissolved in fresh medium, were added every second day. Long-term follow-up of MS-275-treated brain slices revealed a 40% decrease of bulk tumor mass at 12 days after implantation (Fig. 5C) compared with day 1. Tumor mass observed in MS-275-treated slices at day 12 after implantation was >6-fold smaller than in non-treated controls at day 12. Dose escalation to the 5-fold IC_{90} of MS-275 aggravated tumor reduction from 375% in time-matched controls to 32% after treatment compared with day 1 (Fig. 5C). Interestingly, anatomic landmarks within the slice culture, which are helpful to assess its viability (i.e., CA1 pyramidal cell layer and hippocampal fissure), differed between treatment and control paradigms. Severe degeneration occurred only in the untreated group (Fig. 4B), whereas MS-275-treated slice cultures appeared anatomically intact until 12 day *ex vivo* (Fig. 4D).

Blood-Brain Barrier Passage of MS-275

To evaluate whether MS-275 crosses the blood-brain barrier, adult mice were treated with 2 and 4 mg MS-275 by i.p. injection. At 2 and 4 hours after treatment, an accumulation of acetylated H3 core histones was observed in total brain as shown by immunoblot analysis of acetylated versus total histone H3 (Fig. 6A).

MS-275 Blocks Glioma Growth *In vivo*

To confirm the promising results obtained from the organotypic glioma invasion model and to further evaluate the therapeutic efficacy of MS-275, we analyzed the antiglioma action of MS-275 in a syngeneic tumor transplantation model. Whereas control animals bear a median tumor volume of 96 mm^3, tumor masses were reduced significantly to 38 mm^3 in MS-275-treated rats (Fig. 6B and C).

Discussion

Malignant gliomas are common tumors of the central nervous system, but only a minority of patients responds satisfactorily to chemotherapeutic and radiotherapeutic treatment modalities. Progression of malignant gliomas from their ancestor glial precursors might rely on cell-autonomous escape mechanisms for growth arrest and apoptotic cell death (38). These pathogenetic pathways are targeted by mutational hits leading to inactivation of tumor suppressors or activation of oncogenes (39, 40). However, recent evidence also highlights epigenetic dysregulation as important pathomechanisms of cancer (i.e., affecting cell repair circuitries and pathways of programmed cell death; ref. 41). The availability of pharmacologic modifiers for ''epigenetic'' regulation of gene expression (i.e., inhibitors of HDAC) opens new avenues to chemotherapeutic treatment modalities of malignant brain tumors, such as glioblastoma multiforme (WHO grade IV; refs. 5, 13, 42).

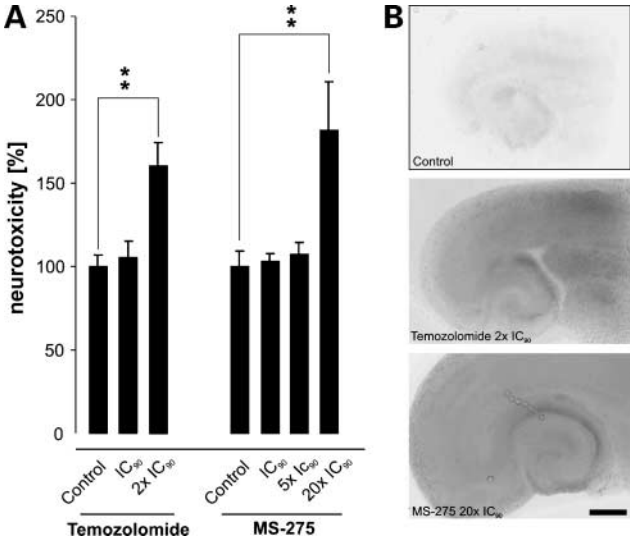

Figure 3. Neurotoxicity of MS-275 and temozolomide. **A,** organotypic entorhino-hippocampal slice cultures were treated with various concentrations of temozolomide or MS-275 for 5 d and neuronal cell damage was scored by PI staining. Significant increase of PI staining was identified for temozolomide at 2-fold IC_{90} concentration, whereas significant PI uptake was registered for MS-275 at 20-fold IC_{90} ($P < 0.01$, t test). **B,** neurotoxicity within brain environment was visualized by fluorescence microscopy. Color images were coded into a gray scale in which higher levels of PI uptake appear darker. Bar, 1 mm.

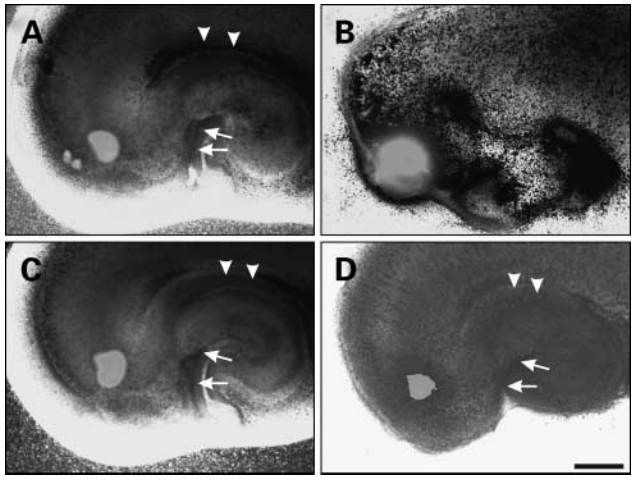

Figure 4. Organotypic glioma invasion model. Enhanced green fluorescent protein – positive F98 glioma cells were transplanted into the entorhinal cortex. Fluorescence microscopic image superimposed onto a translucent image of the same slice culture. **A** and **B,** same slice culture 1 d (**A**) and 12 d (**B**) after tumor implantation. Severe morphologic alterations occurred in the slice architecture after 12 d. **C** and **D,** same slice culture 1 d (**C**) and 12 d (**D**) after tumor implantation and treatment with MS-275 (IC_{90}, 3.75 μmol/L). The bulk tumor mass shrinks and the anatomic slice architecture remains well preserved until 12 d *ex vivo*. Bar, 1 mm.

Recent data obtained from clinical trials using MS-275 for the treatment of cancer show reasonable tolerance after oral application with only moderate side effects (26, 27). Here, we systematically addressed the effect of the benzamide MS-275 to reduce malignant glioma progression *in vitro* (monolayer assay), *ex vivo* (organotypic slice culture), and *in vivo* (tumor transplantation model). Moreover, we identified the propensity of MS-275 to successfully pass the blood-brain barrier. I.p. injection of MS-275 increased the level of acetylated histone H3 protein in brain tissue. Our study highlights, therefore, MS-275 as potent chemotherapeutic drug for the treatment of central nervous system malignancies. As proof-of-concept, the efficacy of MS-275 was compared with that of the DNA alkylating agent temozolomide, which has recently been introduced in the treatment of glioblastoma multiforme and which significantly increase survival time and life quality (24, 25). Calculated equieffective concentrations (IC_{90}) of temozolomide and MS-275 were applied to treat the *ex vivo* organotypic glioma invasion model (35). Both compounds confirmed significant antiglioma properties, and a low neurotoxic potential was discovered for MS-275. Dose escalations were tolerated by the organotypic brain environment up to 20 μmol/L (5-fold IC_{90}), whereas significant cytotoxicity was identified for temozolomide at 2-fold IC_{90} (calculated to be 1.38 mmol/L in our paradigm). Considering that clinical side effects of temozolomide are in a tolerable range (43, 44), MS-275 seems to corroborate a promising perspective in clinical trials. We further employed an *in vivo* model using orthotopic implantation of glioma cells in syngeneic rats followed by a single intratumoral injection of MS-275 7 days later. This experiment confirmed the antiglioma action of MS-275 as described in our *in vitro* and *ex vivo* assays.

Despite the potent antiglioma action in various experimental models, MS-275 was not able to completely inhibit HDAC activity in a cell-free enzymatic assay. Until today, three classes of HDACs have been identified, with only class I and II enzymes being molecular targets of MS-275 (41, 45). According to the Serial Analysis of Gene

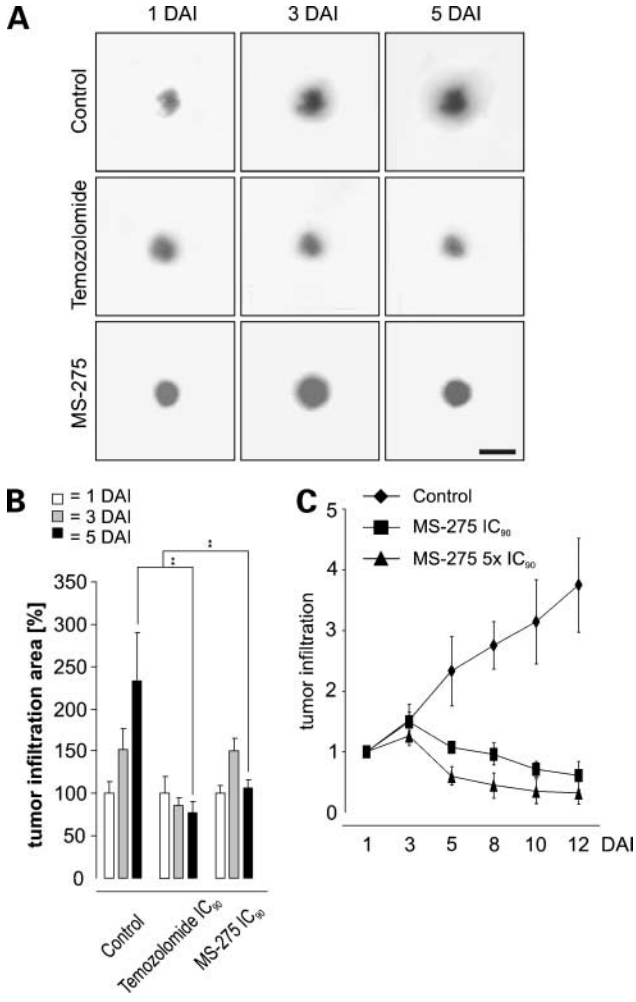

Figure 5. MS-275 reduced tumor growth in the organotypic glioma invasion model. **A,** transplantation of enhanced green fluorescent protein – transfected F98 glioma cells into the entorhinal cortex of the slice culture model and repetitive fluorescent microscopic monitoring. *DAI,* days after implantation. Bar, 450 μm. Slice cultures were treated with equiefficient IC_{90} concentrations of either temozolomide or MS-275. Fluorescence images were not superimposed onto translucent images (see Fig. 4 legend). **B,** tumor infiltration area was measured by analySIS software. *Columns,* mean of nine slice cultures in each group; *bars,* SD. Both compounds significantly reduced tumor growth 5 d after implantation ($P < 0.01$, *t* test). **C,** tumor growth was monitored up to 12 d after implantation. Both concentrations of MS-275 (IC_{90} and 5-fold IC_{90}) reduced tumor growth and reached statistical significance after 5 d after implantation ($P < 0.05$, *t* test).

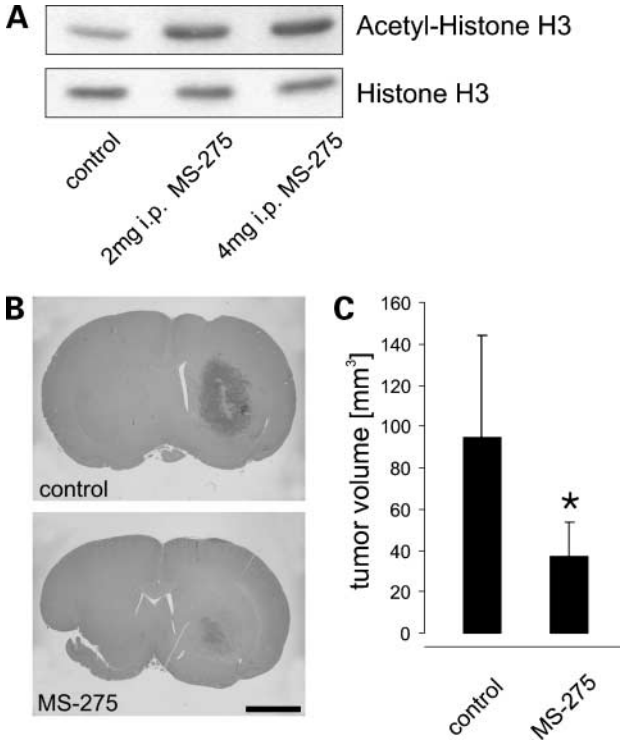

Figure 6. *In vivo* efficacy of MS-275. **A,** MS-275 is able to cross the blood-brain barrier and to increase acetylation of histone H3 already 4 h after i.p. injection into adult mice. **B,** F98 glioma cells were implanted into the right striatum of Fisher rats and a single dose of MS-275 (10 μL of a 10 μmol/L MS-275 solution) or solvent only (10 μL DMSO) was locally given at day 7 after tumor inoculation. **C,** tumor volume was quantified on serial brain sections. *Columns,* mean of six rats in each group; *bars,* SD. MS-275 significantly reduced tumor growth *in vivo* ($P < 0.05$, *t* test).

Expression (46), all class I and II HDAC isoenzymes seem to be expressed in brain. These data are compatible with the notion that favorable antiglioma properties of MS-275 associate with specific inhibition of HDAC isoenzymes (45).

Whereas accumulation of acetylated histones occurs in both normal and transformed cells (47, 48), the low cytotoxicity of HDAC inhibitors in normal compared with neoplastic cells remains enigmatic. Recently, it has been shown that HDAC inhibitors cause an accumulation of reactive oxygen species in transformed but not in normal cells, which is an important resistance determinant observed in native cells and tissues (17, 18). The mechanism of this selectivity remains, however, awaits further studies.

With increasing knowledge that chemotherapy plays a beneficial role in glioma treatment (24, 25), promising data of novel agents, such as HDAC inhibitors, may rapidly translate into clinical trials. However, it is reasonable to suggest that genetic inactivation or activation of key players in neoplastic transformation by allelic loss or mutational hits may induce escape mechanisms also in the face of HDAC inhibitor treatment. To successfully predict chemotherapeutic responsiveness of HDAC inhibitors *in vivo*, molecular diagnostic work-up of tumor specimens will be warranted and remain an important prerequisite to further address the anticancer potency of HDAC inhibitors.

In conclusion, polychemotherapeutic treatment modalities may increase the propensity to pharmacologically challenge highly malignant brain tumors. Adjustment of different treatment modalities, such as combination of DNA alkylating agents with HDAC inhibitors, could be helpful in this respect.

Acknowledgments

We thank T. Jungbauer, B. Rings, and I. Jusen for excellent technical assistance.

References

1. Khochbin S, Verdel A, Lemercier C, Seigneurin-Berny D. Functional significance of histone deacetylase diversity. Curr Opin Genet Dev 2001; 11:162 – 6.

2. de Ruijter AJ, van Gennip AH, Caron HN, Kemp S, van Kuilenburg AB. Histone deacetylases (HDACs): characterization of the classical HDAC family. Biochem J 2003;370:737 – 49.

3. Marks P, Rifkind RA, Richon VM, Breslow R, Miller T, Kelly WK. Histone deacetylases and cancer: causes and therapies. Nat Rev Cancer 2001;1:194 – 202.

4. Lin RJ, Nagy L, Inoue S, Shao W, Miller WH, Jr., Evans RM. Role of the histone deacetylase complex in acute promyelocytic leukaemia. Nature 1998;391:811 – 4.

5. Eyupoglu IY, Hahnen E, Buslei R, et al. Suberoylanilide hydroxamic acid (SAHA) has potent anti-glioma properties *in vitro, ex vivo* and *in vivo*. J Neurochem 2005;93:992 – 9.

6. Rosato RR, Wang Z, Gopalkrishnan RV, Fisher PB, Grant S. Evidence of a functional role for the cyclin-dependent kinase-inhibitor p21WAF1/CIP1/MDA6 in promoting differentiation and preventing mitochondrial dysfunction and apoptosis induced by sodium butyrate in human myelomonocytic leukemia cells (U937). Int J Oncol 2001;19:181 – 91.

7. Kim MS, Blake M, Baek JH, Kohlhagen G, Pommier Y, Carrier F. Inhibition of histone deacetylase increases cytotoxicity to anticancer drugs targeting DNA. Cancer Res 2003;63:7291 – 300.

8. Almenara J, Rosato R, Grant S. Synergistic induction of mitochondrial damage and apoptosis in human leukemia cells by flavopiridol and the histone deacetylase inhibitor suberoylanilide hydroxamic acid (SAHA). Leukemia 2002;16:1331 – 43.

9. Rosato RR, Almenara JA, Grant S. The histone deacetylase inhibitor MS-275 promotes differentiation or apoptosis in human leukemia cells through a process regulated by generation of reactive oxygen species and induction of p21CIP1/WAF1 1. Cancer Res 2003;63:3637 – 45.

10. Richon VM, Sandhoff TW, Rifkind RA, Marks PA. Histone deacetylase inhibitor selectively induces p21WAF1 expression and gene-associated histone acetylation. Proc Natl Acad Sci U S A 2000;97:10014 – 9.

11. Kamitani H, Taniura S, Watanabe K, Sakamoto M, Watanabe T, Eling T. Histone acetylation may suppress human glioma cell proliferation when p21 WAF/Cip1 and gelsolin are induced. Neuro-oncol 2002;4:95 – 101.

12. Komata T, Kanzawa T, Nashimoto T, et al. Histone deacetylase inhibitors, *N*-butyric acid and trichostatin A, induce caspase-8- but not caspase-9-dependent apoptosis in human malignant glioma cells. Int J Oncol 2005;26:1345 – 52.

13. Sawa H, Murakami H, Ohshima Y, et al. Histone deacetylase inhibitors such as sodium butyrate and trichostatin A induce apoptosis through an increase of the bcl-2-related protein Bad. Brain Tumor Pathol 2001;18:109 – 14.

14. Sawa H, Murakami H, Kumagai M, et al. Histone deacetylase inhibitor, FK228, induces apoptosis and suppresses cell proliferation of human glioblastoma cells *in vitro* and *in vivo*. Acta Neuropathol (Berl) 2004;107:523 – 31.

15. Shankar S, Singh TR, Fandy TE, et al. Interactive effects of histone deacetylase inhibitors and TRAIL on apoptosis in human leukemia cells: involvement of both death receptor and mitochondrial pathways. Int J Mol Med 2005;16:1125 – 38.

16. Rahmani M, Yu C, Reese E, et al. Inhibition of PI-3 kinase sensitizes human leukemic cells to histone deacetylase inhibitor-mediated apoptosis through p44/42 MAP kinase inactivation and abrogation of p21(CIP1/WAF1) induction rather than AKT inhibition. Oncogene 2003;22:6231 – 42.

17. Ungerstedt JS, Sowa Y, Xu WS, et al. Role of thioredoxin in the response of normal and transformed cells to histone deacetylase inhibitors. Proc Natl Acad Sci U S A 2005;102:673 – 8.

18. Ruefli AA, Bernhard D, Tainton KM, Kofler R, Smyth MJ, Johnstone RW. Suberoylanilide hydroxamic acid (SAHA) overcomes multidrug resistance and induces cell death in P-glycoprotein-expressing cells. Int J Cancer 2002;99:292 – 8.

19. Bali P, Pranpat M, Swaby R, et al. Activity of suberoylanilide hydroxamic Acid against human breast cancer cells with amplification of HER-2. Clin Cancer Res 2005;11:6382 – 9.

20. Acharya MR, Figg WD. Histone deacetylase inhibitor enhances the anti-leukemic activity of an established nucleoside analogue. Cancer Biol Ther 2004;3:719 – 20.

21. Stewart LA. Chemotherapy in adult high-grade glioma: a systematic review and meta-analysis of individual patient data from 12 randomised trials. Lancet 2002;359:1011 – 8.

22. DeAngelis LM. Brain tumors. N Engl J Med 2001;344:114 – 23.

23. Laws ER, Parney IF, Huang W, et al. Survival following surgery and prognostic factors for recently diagnosed malignant glioma: data from the Glioma Outcomes Project. J Neurosurg 2003;99:467 – 73.

24. Stupp R, Mason WP, van den Bent MJ, et al. Radiotherapy plus concomitant and adjuvant temozolomide for glioblastoma. N Engl J Med 2005;352:987 – 96.

25. Wick W, Steinbach JP, Kuker WM, Dichgans J, Bamberg M, Weller M. One week on/one week off: a novel active regimen of temozolomide for recurrent glioblastoma. Neurology 2004;62:2113 – 5.

26. Ryan QC, Headlee DJ, Sparreboom A, et al. A phase I trial of an oral histone deacetylase inhibitor, MS-275, in advanced solid tumor and lymphoma patients. ASCO Annu Meet; 2003 May 31-Jun 3; Chicago, IL.

27. Wisinski KB. A phase I study of an oral histone deacetylase inhibitor, MS-275 in patients with refractory solid tumors and lymphoma. Proc Am Soc Clin Oncol 2003.

28. Ko L, Koestner A, Wechsler W. Morphological characterization of nitrosourea-induced glioma cell lines and clones. Acta Neuropathol (Berl) 1980;51:23 – 31.

29. Ponten J, Macintyre EH. Long term culture of normal and neoplastic human glia. Acta Pathol Microbiol Scand 1968;74:465 – 86.

30. Benda P, Lightbody J, Sato G, Levine L, Sweet W. Differentiated rat glial cell strain in tissue culture. Science 1968;161:370 – 1.

31. Sampson JH, Ashley DM, Archer GE, et al. Characterization of a spontaneous murine astrocytoma and abrogation of its tumorigenicity by cytokine secretion. Neurosurgery 1997;41:1365 – 72; discussion 1372 – 3.

32. Heltweg B, Jung M. A microplate reader-based nonisotopic histone deacetylase activity assay. Anal Biochem 2002;302:175 – 83.

33. Eyupoglu IY, Bechmann I, Nitsch R. Modification of microglia function protects from lesion-induced neuronal alterations and promotes sprouting in the hippocampus. FASEB J 2003;17:1110 – 1.

34. Stoppini L, Buchs PA, Muller D. A simple method for organotypic cultures of nervous tissue. J Neurosci Methods 1991;37:173 – 82.

35. Eyupoglu IY, Hahnen E, Heckel A, et al. Malignant glioma-induced neuronal cell death in an organotypic glioma invasion model [technical note]. J Neurosurg 2005;102:738 – 44.

36. Fulda S, Wick W, Weller M, Debatin KM. Smac agonists sensitize for Apo2L/TRAIL- or anticancer drug-induced apoptosis and induce regression of malignant glioma *in vivo*. Nat Med 2002;8:808 – 15.

37. Saito A, Yamashita T, Mariko Y, et al. Synthetic inhibitor of histone deacetylase, MS-27-275, with marked *in vivo* antitumor activity against human tumors. Proc Natl Acad Sci U S A 1999;96:4592 – 7.

38. Maher EA, Furnari FB, Bachoo RM, et al. Malignant glioma: genetics and biology of a grave matter. Genes Dev 2001;15:1311 – 33.

39. Reifenberger G, Louis DN. Oligodendroglioma: toward molecular definitions in diagnostic neuro-oncology. J Neuropathol Exp Neurol 2003;62:111 – 26.

40. von Deimling A, Louis DN, Wiestler OD. Molecular pathways in the formation of gliomas. Glia 1995;15:328 – 38.

41. Marks PA, Richon VM, Miller T, Kelly WK. Histone deacetylase inhibitors. Adv Cancer Res 2004;91:137 – 68.

42. Marks PA, Richon VM, Rifkind RA. Histone deacetylase inhibitors: inducers of differentiation or apoptosis of transformed cells. J Natl Cancer Inst 2000;92:1210 – 6.

43. Yung WK, Albright RE, Olson J, et al. A phase II study of temozolomide vs. procarbazine in patients with glioblastoma multiforme at first relapse. Br J Cancer 2000;83:588 – 93.

44. Khan RB, Raizer JJ, Malkin MG, Bazylewicz KA, Abrey LE. A phase II study of extended low-dose temozolomide in recurrent malignant gliomas. Neuro-oncol 2002;4:39 – 43.

45. Hu E, Dul E, Sung CM, et al. Identification of novel isoform-selective inhibitors within class I histone deacetylases. J Pharmacol Exp Ther 2003; 307:720 – 8.

46. Lash AE, Tolstoshev CM, Wagner L, et al. SAGEmap: a public gene expression resource. Genome Res 2000;10:1051 – 60.

47. Butler LM, Agus DB, Scher HI, et al. Suberoylanilide hydroxamic acid, an inhibitor of histone deacetylase, suppresses the growth of prostate cancer cells *in vitro* and *in vivo*. Cancer Res 2000;60: 5165 – 70.

48. Kelly WK, Richon VM, O'Connor O, et al. Phase I clinical trial of histone deacetylase inhibitor: suberoylanilide hydroxamic acid administered intravenously. Clin Cancer Res 2003;9:3578 – 88.